

**Investigations into the Reactivity of an Early/Late Zr/Co  
Heterobimetallic with Pyrazine Derivatives**

Senior Thesis

Presented to

The Faculty of the School of Arts and Sciences

Brandeis University

Undergraduate Program in Chemistry

Professor Christine M. Thomas (Advisor)

In Partial Fulfillment of the Requirements for the Degree of Bachelor of Arts

By Ben Crown

May 2013

Copyright by

Ben Crown

## Acknowledgements

First I would like to thank Christine Thomas, who made all of this possible by allowing me to volunteer in her lab fresh out of general chemistry in the summer after my freshman year and gave me this interesting project that culminated in this thesis. I'd like to thank Wes, who took the time out of his busy grad student life to sit me down and teach me some organic and inorganic chemistry (You were and continue to be a great teacher). And I did love hearing the song you heard on the radio each morning, repeatedly. I'd like to thank Seth, who helped greatly in guiding me through how to approach this thesis and really made me think more critically about my work and the timeframe I had to work with (writing this would have been a lot messier had I not gotten such a good head start on it). I'd also like to thank both Jeremy (for the sound track, both from the pentane sub and Jeremy covers) and Kuppu for always being there to help me with whatever my chemistry was throwing at me that day, you both had a solution for any situation I could manage to get myself into in 316. Mark and Bruce Foxman also deserve a lot of thanks for their great efforts in helping me with all my crystallography. Without Mark's determination to find a usable crystal, who knows if I would have the structure of the pyridine compound (I certainly wouldn't have such a shiny picture of it without him). Thank you to Deirdra, Wen, Bing, Saddle, and Ramyaa because I had enough questions for everyone and you all were there to offer support. Thank you to all the undergrads for being such great labmates. I'd like to thank my whole Mod, extended Mod family, Jess, Jake, Brad, and my friends for listening to me complain about the stresses of my thesis and for always being supportive and letting me get my work done before shenanigans. Finally I'd like to thank my family for all of their support and letting me take the car to get to the lab so many days. I have the utmost appreciation for all of the help I have received in the Thomas lab. I am convinced that there isn't a better lab out there for a young chemistry undergrad to make their start in and I was lucky to be a part of it.

## Table of Contents

Abstract	4
Introduction	5
Early/Late Heterobimetallics and the Zr/Co Heterobimetallic	5
Observed Reactivity of Zr/Co Heterobimetallic	8
Pyrazine and Charge Transfer	11
Radical Reactivity of Pyrazine Derivatives	12
Investigative Approach	15
Results and Discussion	17
Orbital Energies via Density Functional Theory Calculations	22
Potential products of the Pyrazine Reaction	24
Conclusion	27
Experimental	28
References	32

## Abstract

The electronic properties of the unstable product of a Zr/Co heterobimetallic complex and pyrazine are explored by trying to emulate the observed charge transfer in similar reactions with several pyrazine derivatives. A series of products are proposed that demonstrate simple ligand exchange and fail to recreate the observed charge transfer but are informative about what is required to induce charge transfer and the steric constraints of a reaction. Orbital energies are calculated using density functional theory, showing that pyrazine's low energy  $\pi$  orbitals are what facilitate the charge transfer. Speculation into the unstable species that produces the charge transfer leads to a dichotomy between a bridging pyrazine species or a ligand exchange product, which hinges on the steric restrictions of the reaction.

## Introduction

Bimetallic chemistry is defined as chemical reactions where two elements other than those in the main group cooperate in stoichiometric or catalytic reactions.<sup>1</sup> The crux of bimetallic catalysis is the cooperative reactivity between the metal centers and the underlying coordination chemistry that directly affects their properties. Various types of ligands impart differing effects on the metal centers; the ligands have important applications in manipulating the coordination sphere to obtain high selectivity in catalytic reactions.<sup>2</sup> Binuclear compounds are known to have notably different reactivity from their mononuclear analogs. In the area of bimetallic chemistry, the use of two very different metals has become an area of interest, as it leads to the greatest modification of reactivity over mononuclear analogues.<sup>2</sup>

### Early/Late Heterobimetallics and the Zr/Co Heterobimetallic

The use of an early and a late transition metal in a heterobimetallic complex promotes unique cooperative reactivity that allows these complexes to activate many small molecules.<sup>2,3,4</sup> The nature of the metal-metal interaction is centered around the different electronic properties of the two metals: the early metal is hard and Lewis acidic while the late metal is soft and Lewis basic ( $M_1$  and  $M_2$  respectively in Figure 1). The combination of these types of metal centers yields a dative interaction, where the electron-poor early metal draws electron density from the electron-rich late metal. This electronic character has a significant effect on the redox activity of the metals, which can potentially allow these complexes to reduce or oxidize a substrate at more mild potentials than a comparable homobimetallic complex.<sup>3</sup> Another characteristic of these

compounds is the polar nature of the metal-metal bond, which has the potential to facilitate heterolytic activation of substrates across the bond (Figure 1).<sup>3</sup>

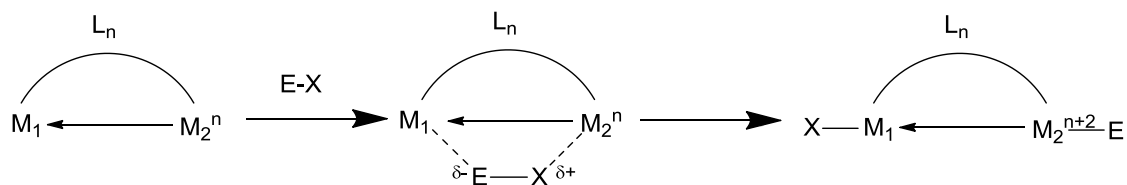


**Figure 1.** A general mechanism of heterolytic activation of substrates (E-X) across the metal-metal bond of early/late heterobimetallic compounds.

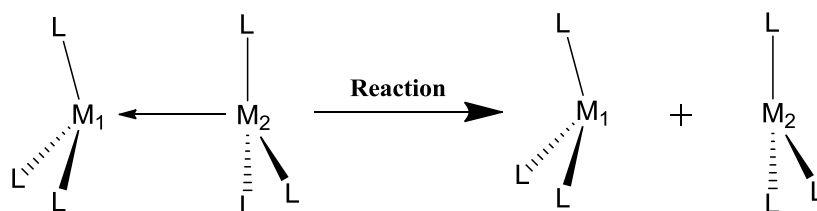
When considering heterobimetallics, it is critical to consider the structural, steric, and electronic implications of the ligands that bridge the metal centers. Without these crucial bridging structures, the metal-metal bond will commonly break upon reactivity with small molecules, making the system react like a 1:1 mixture of the monometallic species (seen in Figure 2).<sup>3</sup> When selecting a ligand system, it is important to consider its steric bulk and whether there is adequate space for substrates to reach the reactive site of the catalyst.<sup>3</sup> The strength of the metal-ligand bonds is also significant, as more labile ligands can be displaced or shifted to the other metal, facilitating the access of substrates to the polar metal-metal bond (summarized in Figure 2).<sup>3</sup>

The ligand system that we have chosen to use for much of our heterobimetallic chemistry is an LX-type phosphinoamide linker ( $[\text{Ph}_2\text{PNR}]^-$ , R = 2,4,6-trimethylphenyl, <sup>t</sup>Bu or <sup>i</sup>Pr).

Nagashima et al. worked with titanium and zirconium complexes supported by phosphinoamides and have shown that these compounds can function as metalloligands towards late transition metals ( $\text{Cu}^{\text{I}}$ ,  $\text{Mo}^0$ ).<sup>5,6</sup> The ligand system allows for the tuning of steric properties at the early metal by changing the substituents on the amides and phosphines. The electronic properties are also conducive to early/late heterobimetallic complexes, as the X-type amides are bound to the

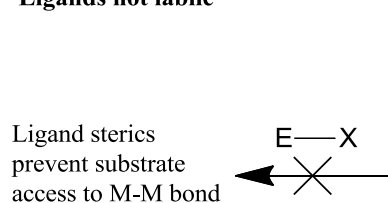
early metal, increasing its oxidation state and thus strengthening its interaction with the electron rich metal. Meanwhile, the L-type phosphines are bound to the electron rich late metal, further supplying it with electrons that can be donated to the early metal. These electronic properties contribute to more mild reduction potentials for the complex, facilitating reactivity. Another advantage of this type of ligand is that the 2-atom bridging system allows  $\eta^2$  coordination at one metal center, facilitating the hemilability that allows the ligand to flip to one metal and open the active site of the catalyst to the substrate, thus leading to increased reactivity at the metal-metal bond (seen in Figure 2).<sup>3</sup>

### Reactivity of Metal-Metal Interactions without Supporting Ligand Structure



### Metals Linked by Bridging Ligands

**Ligands not labile**



**L<sub>1</sub> is a labile ligand**

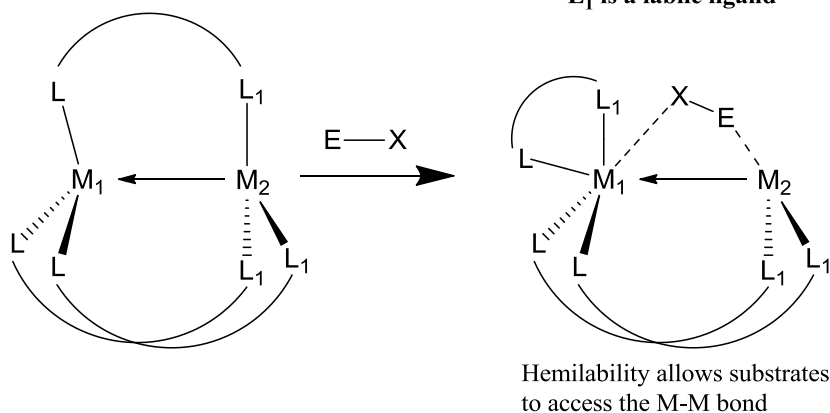
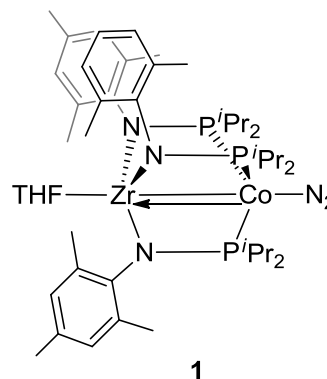


**Figure 2.** An overview of the significance and implications of ligand support and lability in early/late heterobimetallic compounds.<sup>3</sup>

The metals in a bimetallic compound can directly affect each other's properties if the distance between them is short enough to allow it. This interaction can either be described as

covalent, where each of the electron pairs being shared would otherwise be unpaired on their respective metal, or dative, where a pair of nonbonding electrons is donated from one metal to the other.<sup>2</sup> One heterobimetallic complex that has been of interest to our group for several years is

(THF)Zr(MesNP<sup>i</sup>Pr<sub>2</sub>)<sub>3</sub>CoN<sub>2</sub> (**1**, Mes = 2,4,6-trimethylphenyl),

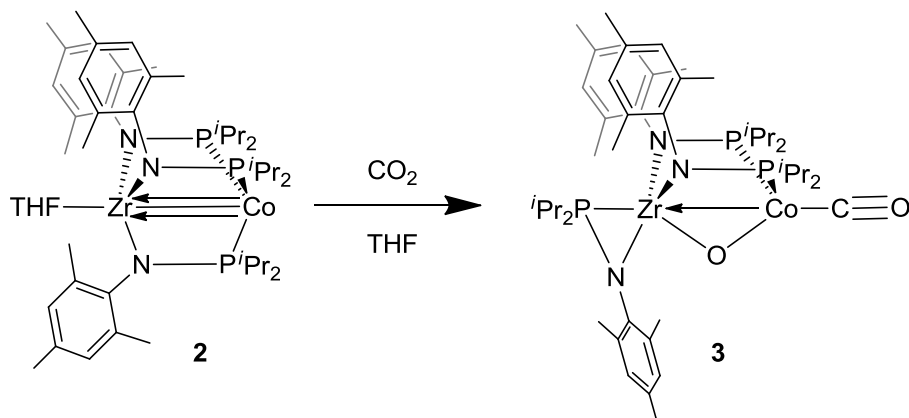


which features well-characterized metal-metal bonding, three phosphinoamide bridging ligands, and labile THF and N<sub>2</sub> ligand.<sup>3,5,7</sup> X-ray crystallography shows that **1** has a Zr/Co bond distance of 2.33 Å, which is significantly less than the sum of the covalent radii of Zr and Co (approximately 1.75 Å and 1.26 Å respectively).<sup>7,8</sup> The short bond distance reflects the metal-metal interaction that occurs: the metals have formed a metal-metal bond and the electron rich Co donates electrons to the electron poor Zr through their overlapping d<sub>22</sub> orbitals (supported by DFT calculations).<sup>3</sup> The electron donation from the filled Lewis basic Co d<sub>22</sub> orbital to the empty Lewis acidic Zr d<sub>22</sub> orbital yields a dative bonding interaction. This Zr/Co heterobimetallic has been shown to have reactivity with several small molecules substrates such as CO<sub>2</sub><sup>9</sup> dihydrogen,<sup>10</sup> alkyl halides,<sup>10</sup> and hydrazine.<sup>11</sup>

### Observed Reactivity with the Zr/Co Heterobimetallic

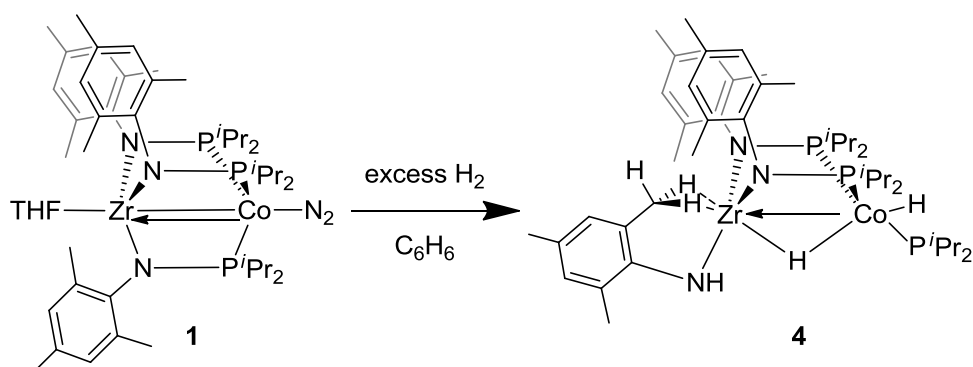
Experiments with CO<sub>2</sub> have shown that the high polarity of the Zr/Co multiple bond in compound **2** ((THF)Zr(MesNP<sup>i</sup>Pr<sub>2</sub>)<sub>3</sub>Co) allows for the facile oxidative addition of the carbonyl in CO<sub>2</sub> to produce a terminal CO on Co and a bridging oxo moiety between the metal centers, as seen in (OC)Co(MesNP<sup>i</sup>Pr<sub>2</sub>)<sub>2</sub>-(μ-O)Zr(MesNP<sup>i</sup>Pr<sub>2</sub>) (compound **3**) in Scheme 1.<sup>9</sup> The key to the reactivity is the hemilability of the phosphinoamide ligand system, as the phosphine dissociates from the Co center and binds to Zr in a bidentate fashion, allowing the CO<sub>2</sub> to access the metal-

metal bond.<sup>9</sup> This transformation is impressive, as the strength of C=O bonds in CO<sub>2</sub> (bond dissociation energy: 525.9±0.4kJ/mol)<sup>13</sup> is enough to prevent reactivity with most compounds.



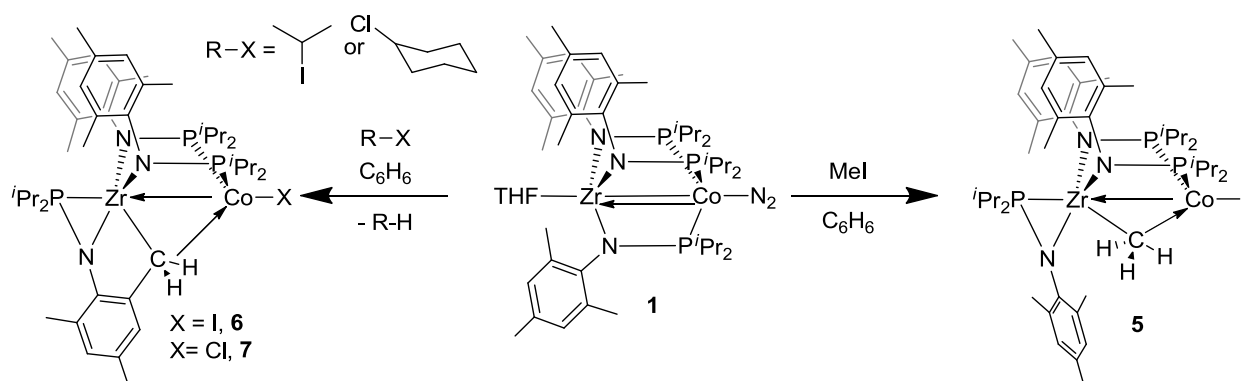
**Scheme 1.** Reactivity of complex **2** with CO<sub>2</sub>.

Upon adding excess H<sub>2</sub> to compound **1** (with dinitrogen removed via vacuum), two equivalents of H<sub>2</sub> are consumed via oxidative addition to form compound **4**, seen in Scheme 2.<sup>10</sup> The P-N bond of one of the bridging ligands has been broken to generate a secondary phosphine ligand on the Co and a terminal Zr amide. The second equivalent of H<sub>2</sub> generates a bridging hydride between the metal centers and a terminal Co-H. This chemistry is the first known example of H<sub>2</sub> causing P-N bond cleavage.<sup>3,10</sup>



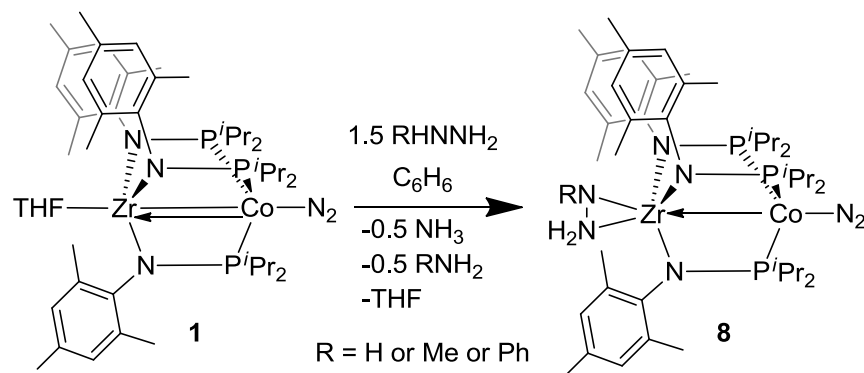
**Scheme 2.** Reactivity of complex **1** with H<sub>2</sub>.

Compound **1** has been shown to have varying reactivity with different alkyl halides. Treatment of **1** with MeI forms compound **5** (seen in Scheme 3), in which the I<sup>-</sup> binds to Co terminally and the methyl group is shown to add to the Co-Zr bond and generate a bridging methyl group. Again, a P donor from one of the phosphinoamide ligands has dissociated from the Co center to coordinate to Zr.<sup>10</sup> The addition of iodopropane or cyclohexyl chloride to compound **1** did not yield a similar bridging species, but instead an intramolecular C-H activation product<sup>10</sup> (**6** and **7**, respectively, seen in Scheme 3). Due to the relative rarity of alkyl halide activation, this reactivity was applied to catalysis, specifically Kumada coupling.<sup>12</sup>



**Scheme 3.** Reactivity of complex **1** with several alkyl halides.

When compound **1** is treated with a hydrazine RNHNH<sub>2</sub>, it undergoes a one-electron oxidative addition where the N-H bond is broken in order to form the  $\eta^2$ -hydrazido ligand on the Zr center seen in compound **8** (Scheme 4).<sup>11</sup> It is uncommon for both N-H activation to occur at an early metal, and for Zr to participate in one-electron chemistry. The corresponding amine RNH<sub>2</sub> and ammonia are generated as byproducts of the hydrogen atom transfer involved in the hydrazine activation.<sup>11</sup>



**Scheme 4.** Reactivity of complex **1** with hyrazine derivatives.

### Pyrazine and Charge Transfer

Another small molecule of interest is pyrazine, as it is readily able to bind at either nitrogen atom, making it a common reagent for the formation of dimers or bridged compounds,<sup>14,15</sup> and as a spacer in coordination polymers.<sup>16</sup> In order to assess the properties of analogues of complex **1** in dimer or polymer form, the Zr/Co heterobimetallic complex was treated with pyrazine, immediately adopting a vivid blue coloration with visibly high molar absorptivity, potentially alluding to radical chemistry or charge transfer of some kind. Because Since charge transfer properties have several important applications, further study of the compound was pursued.

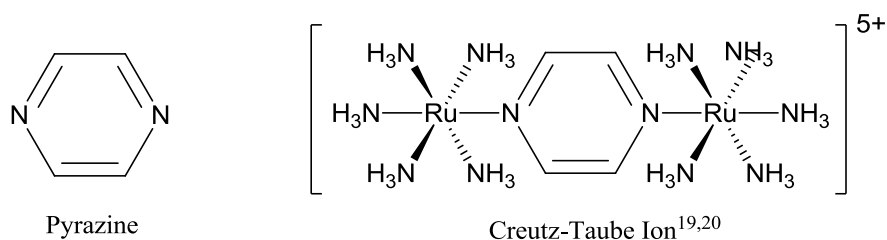


**Chart 1.** Pyrazine and the Creutz-Taube ion, one of the first mixed-valence complexes synthesized, featuring a bridging pyrazine ligand between two ruthenium ions.<sup>19,20</sup>

The unique electronic properties of charge transfer complexes can yield metal-like conductivity, allowing for applications in various electronic devices such as transistors and solar

cells.<sup>17</sup> Mixed valence compounds also exhibit charge transfer, as participating elements simultaneously exist in more than one oxidation state as electrons are delocalized throughout the molecule.<sup>18</sup> Around 1970, one of the first mixed-valence complexes was synthesized: a  $\mu$ -pyrazine dimer species referred to as the "Creutz-Taube ion,"  $[(\text{NH}_3)_5\text{Ru}(\text{pz})\text{Ru}(\text{NH}_3)_5]^{5+}$  (Chart 1, pz = pyrazine).<sup>19,20</sup> The ion demonstrates pyrazine's ability to electronically couple two metals indirectly by mixing metal-based donor and acceptor orbitals with its own orbitals that are of the proper symmetry.

The aromatic nature of pyrazine gives it the potential to provide stability to otherwise very reactive radicals; however, this effect is limited by its relatively small size. Despite this shortcoming, pyrazine has been reported to form a radical anionic species that can bridge metals such as Be, Mg or Zn.<sup>21</sup> In addition to the pyrazine species, 4,4'-bipyridine radical anions have also been synthesized and treated with Group IV carbonyl compounds such as  $\text{Mo}(\text{CO})_6$  and  $\text{W}(\text{CO})_6$  to form bridged anionic radical dimer species.<sup>22</sup> A radical dimer is a reasonable hypothesis for the observed reaction between compound **1** and pyrazine, although observed radical chemistry with the Zr/Co heterobimetallic complex suggest an alternative radical mechanism.

### Radical Reactivity of Pyrazine Derivatives

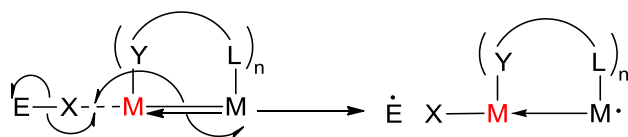
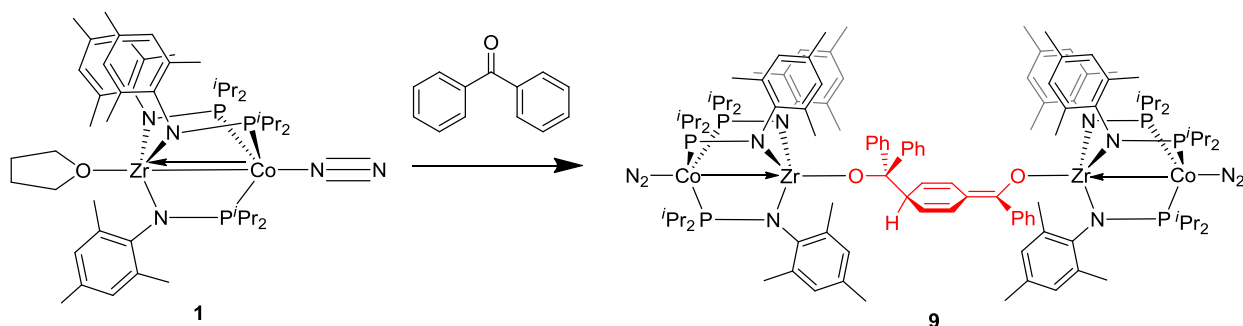


**Figure 3** shows a mechanism for forming a ligand based radical through homolytic cleavage of the metal-metal bond.

As seen in Figure 3, the proposed radical mechanism shows the formation of a metal-ligand bond inducing a homolytic cleavage of the metal-metal bond, which results in the

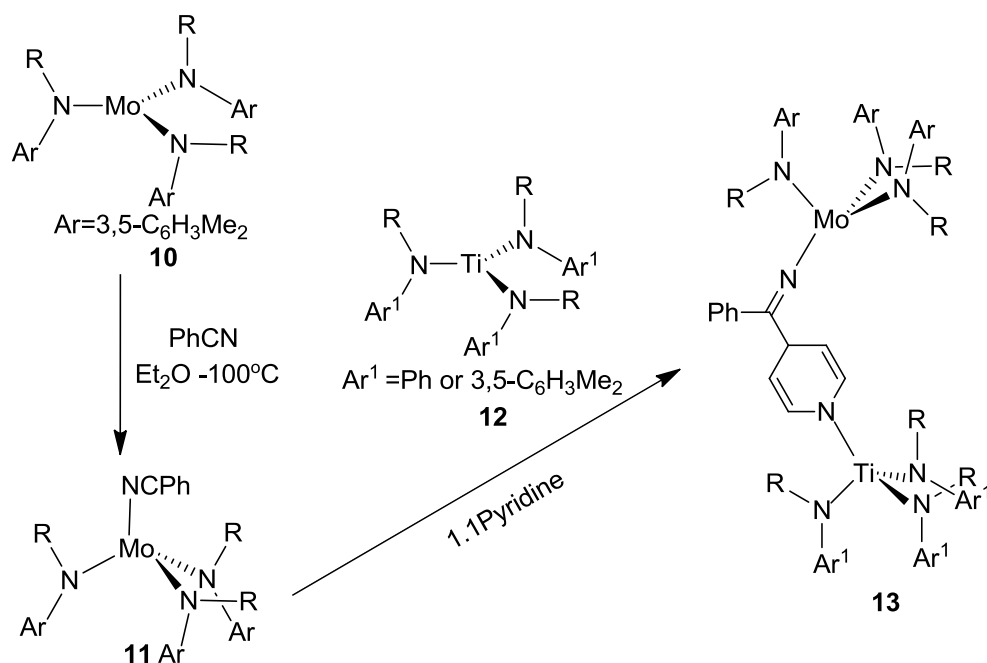
formation of a reactive ligand-based radical and transfer of an electron to the metal. The radical process has recently been reported by Zhou and Marquard *et al.*; the report elucidates the reaction between the Zr/Co heterobimetallic complex **1** and benzophenone.<sup>23</sup> Benzophenone binds to the electron-poor Zr center, causing homolytic cleavage of the metal-metal bond, which induces electron transfer to the cobalt and forms a stabilized ligand-based ketyl radical on the Zr-benzophenone unit. The ligand is able to stabilize the radical by delocalizing the charge in its two aromatic rings. Over time, radical coupling of two ketyl radical fragments from separate molecules yields an asymmetric tetrametallic dimer (compound **9**, Scheme 5). The reaction would be more favorable if not for the loss of aromaticity that occurs on the central phenyl ring. The coupling occurs between the carbonyl carbon atom of one ligand, as it is the primary location of the spin density (according to computational results), and the *para* carbon of one of the phenyl rings on the other benzophenone molecule.<sup>23</sup> The reactivity of the pyrazine or pyridine could operate under a similar radical mechanism, although these molecules are less effective at radical stabilization than such a large conjugated pi-system.



**Scheme 5.** Radical dimerization reaction that occurs upon treatment of **1** with benzophenone.<sup>23</sup>

Mendiratta *et al.* reported heterobimetallic reductive cross-coupling of benzonitrile with carbon dioxide, pyridine, and benzophenone (Scheme 6).<sup>24</sup> Benzonitrile coordinates to the Mo(III) center of compound **10**, oxidizing the metal and forming the somewhat stable

molybdenum-benzonitrile radical adduct (**11**) *in situ*; the resultant complex may be described as a long lived intermediate. At  $-100\text{ }^{\circ}\text{C}$  in  $\text{Et}_2\text{O}$ , complex **11** is mixed with the Ti(III) compound **12**, immediately followed by the addition of a substrate, such as pyridine. The pyridine oxidizes the Ti(III) center and forms a pyridinyl radical that readily couples to the radical adduct **11** through the *para* carbon atom, producing a new C-C bond as the electrons are paired. In turn, a comparable reaction can be observed with  $\text{CO}_2$  or benzophenone in place of the pyridine to undergo analogous radical cross coupling and bond formation.<sup>24</sup>



**Scheme 6.** Radical coupling to a Mo-benzonitrile radical adduct and pyridine in the presence of Ti(III) forming a new C-C bond.<sup>24</sup>

Between the radical mechanism observed by Zhou and Marquard *et al.*<sup>23</sup> and the radical-based reductive cross coupling observed by Mendiratta *et al.*,<sup>24</sup> there is some room for educated speculation into the reactivity between the Zr/Co heterobimetallic **1** and pyrazine and pyrazine derivatives. The homolytic cleavage of the Zr-Co bond that places the radical on the benzophenone moiety to create the ligand-based radical could also be part of the mechanism for

the pyrazine reaction. The observation that pyridine participates in this radical cross coupling reaction shows its ability to potentially accept a radical from a metal center, providing some prospective evidence that pyrazine, being an analogue of pyridine, could also accept a radical. However, it is likely that pyrazine and derivatives of a similar size would not sufficiently stabilize a radical due to their relatively small aromatic systems, which would likely prevent adequate delocalization of spin density.

### Investigative Approach

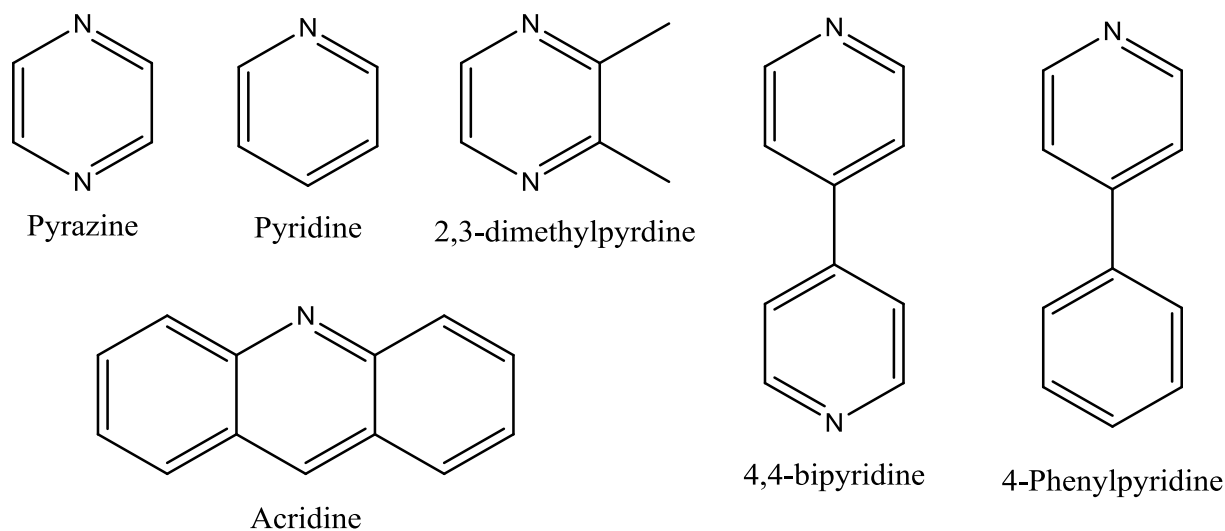
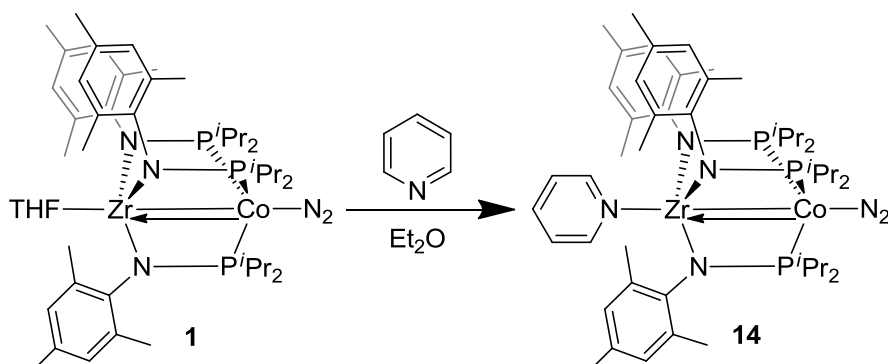


**Chart 2.** Pyrazine and relevant derivatives.

In order to investigate this potentially radical mechanism, we proposed to react compound **1** with pyrazine, pyridine, 2,3-dimethyl pyrazine, acridine, 4,4'-bipyridine, and 4-phenylpyridine. Each compound should help provide evidence for or against the radical mechanism. Pyridine removes the element of the second nitrogen, potentially reacting similarly to pyrazine without the ability to dimerize or polymerize through the nitrogen. 2,3-dimethyl pyrazine leaves the element of the second nitrogen, but adds steric bulk that could either prevent

the potential radical activity observed or react very similarly to pyrazine depending on the mechanism. Acridine and 4,4'-bipyridine are notably more bulky and feature large aromatic pi-systems that are planar and (possibly) non-planar respectively, which should be more likely to maintain a stable ligand-based radical owing to their increased ability to delocalize the charge. Acridine should behave more like pyridine as it also lacks the second nitrogen atom, while 4,4'-bipyridine should behave more like pyrazine since it has the ability to bind through the second nitrogen and potentially bridge between the bimetallic complexes. The 4-phenylpyridine should react similarly to the pyridine, but the electron-withdrawing substituent may result in increased electron donation from the metal and allow for improved electron delocalization. By exploring the reactivity between compound **1** and pyrazine and several derivatives, the observed products will either be consistent with the radical mechanism suggested or reflect an alternate mechanism that may explain the hypothesized charge transfer.

## Results and Discussion



**Scheme 7.** The reaction between compound **1** and pyridine in Et<sub>2</sub>O yielded compound **14**. This structure was confirmed via single crystal X-ray diffraction.

A 1:1 mixture of compound **1** and pyridine was reacted in diethyl ether at room temperature. The THF on complex **1** was displaced by pyridine, producing compound **14** in a 72.4 % yield (seen in Scheme 7); the structure was confirmed by single crystal X-ray diffraction (seen in Figure 4). This substitution demonstrates that pyridine is the favored ligand owing to its slightly greater ability to donate electrons to Zr. This property is reflected in a very slight elongation in the Zr–Co interatomic distance from 2.3683(9) Å in compound **1** and 2.3738(2) Å seen in compound **14**.<sup>7</sup> It should be noted that the bound pyridine was not readily observable using <sup>1</sup>H NMR spectroscopy, but was merely a broad peak in the aromatic region, which suggests some sort of fluxional behavior in the binding of pyridine to the Zr Center.

The observed pyridine–Zr bond distance is 2.503(1) Å, which is slightly longer than other observed Zr(IV)–pyridine bond distances: 2.412 Å<sup>25</sup>, 2.487 Å.<sup>26</sup> The difference may be explained by steric effects arising from pyridine's proximity to the mesityl ring systems, or by the Zr center having more electron density than the typical Zr(IV) ion due to donation of electron density from the Co center. The structure of compound **14** also shows that pyridine is likely involved in a  $\pi$ -stacking interaction with one of the mesityl ring systems, which is most readily observable in

Figure 4 as a slight deviation from a linear  $\text{Co}_1\text{-Zr}_1\text{-N}_6$  bond angle ( $\text{Co}_1\text{-Zr}_1\text{-N}_6$  bond angle =  $171.98(2)$ ).

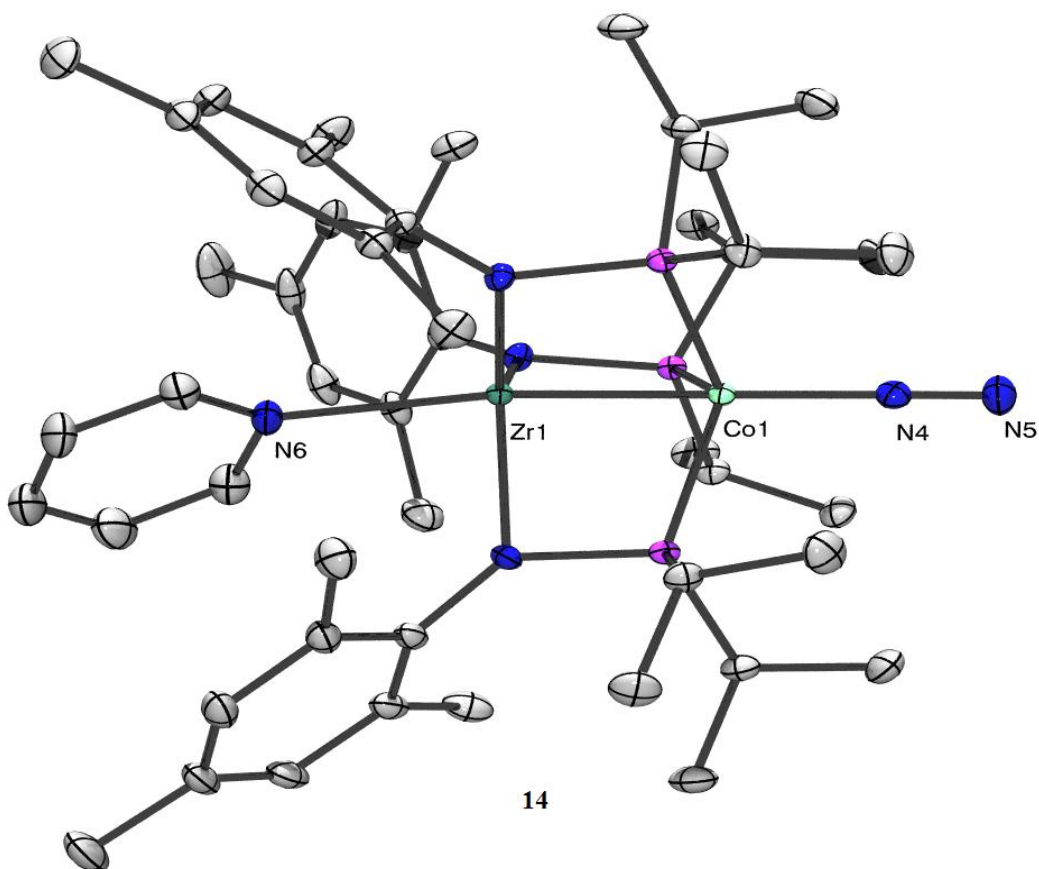
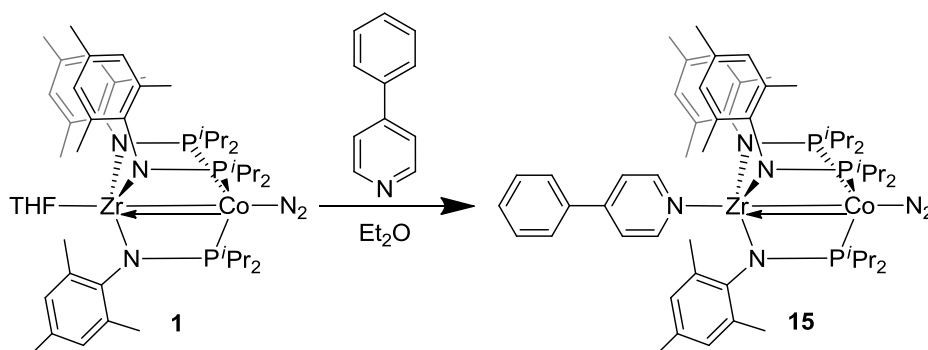


**Figure 4.** The structure of compound **4** was obtained via x-ray crystallography. Displacement ellipsoids (50% probability). All hydrogen atoms are omitted for clarity. Relevant interatomic distances (Å): N6–Zr, 2.5035(10); Zr–Co, 2.3738(2); Co–N4, 1.8248(10); N4–N5, 1.1211(14).

The result does not fit the radical mechanism previously suggested by the chemistry observed by Zhou and Marquard *et al.*<sup>23</sup> involving ligand-based radical formation from homolytic bond cleavage. This is likely because of the pyridine ligand's insufficient reduction potential (preventing it from favorably accepting an electron) and also its inability to stabilize such a reactive radical species; pyridine is too small and unable to adequately delocalize the charge like benzophenone. However, larger aromatic pyridine derivatives such as acridine and 4-phenylpyridine are more likely to sufficiently stabilize a ligand-based radical. The 1:1 reaction

between compound **1** and acridine was run in diethyl ether at room temperature and no reaction was observed by  $^1\text{H}$  NMR spectroscopy. The lack of reactivity is likely caused by the steric hindrance from the large mesityl groups, which prevents the acridine from interacting with the early metal. The steric issues should be overcome by the use of the less bulky derivative 4-phenylpyridine.

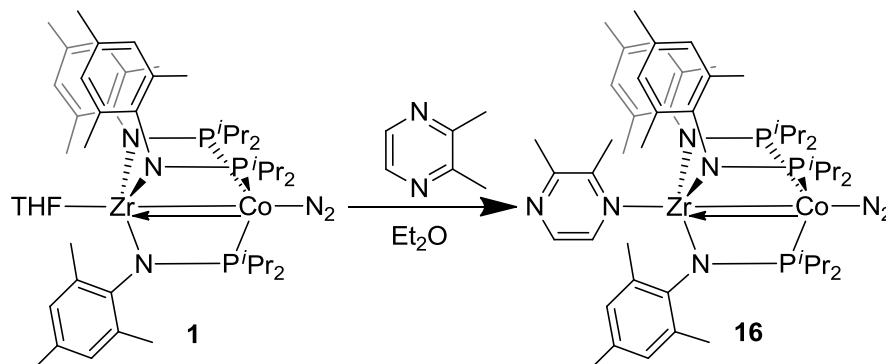


**Scheme 8.** The reaction between compound **1** and 4-phenylpyridine in  $\text{Et}_2\text{O}$  likely forms structure **15** because of comparable  $^1\text{H}$  NMR data to compound **14**.

Compound **1** was exposed to 4-phenylpyridine in a 1:1 ratio in diethyl ether at room temperature, instantly causing the crystallization of compound **15**. The  $^1\text{H}$  NMR spectrum of the compound was found to be very similar to that of compound **14**. The clear similarities suggest analogous connectivity of the 4-phenylpyridine to the Zr center in compound **15**. The 4-phenylpyridine moiety was only observable spectroscopically as a broad peak in the aromatic region, suggesting a comparable fluxional process to that seen with pyridine. The electron-withdrawing abilities of the phenyl group on the pyridine lowers the orbital energies, allowing 4-phenylpyridine to more readily accept and delocalize electrons compared to pyridine. It was thought that this property may have been able to either (a) allow for the progression of the proposed radical mechanism with homolytic cleavage of the metal-metal bond, or (b) facilitate more charge transfer than the pyridine analogue and more closely emulate the chemistry seen

with the pyrazine. However, both theories were found to be unsupported, as it seems that the 4-phenylpyridine ligand behaves much like pyridine as it substitutes THF on the Zr center.

Because pyrazine derivatives that lacked the second nitrogen in the ring seemed to behave much differently than pyrazine, derivatives were explored that could utilize this additional nitrogen such as 2,3-dimethyl pyrazine.

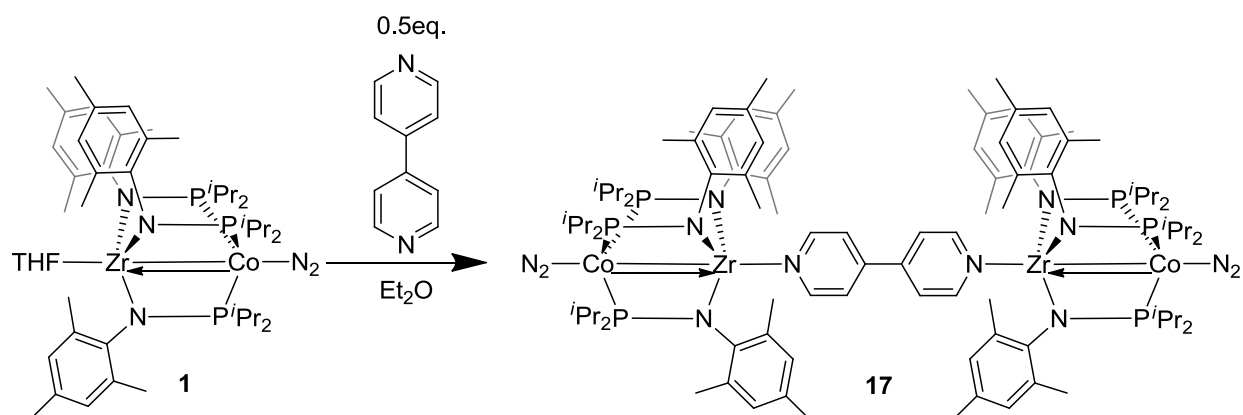


**Scheme 9.** The reaction between compound **1** and 2,3-dimethyl pyrazine in Et<sub>2</sub>O forms the proposed structure of compound **16**, as <sup>1</sup>H NMR data suggests connectivity similar to complex **14**.

A 1:1 reaction of compound **1** and 2,3-dimethylpyrazine was run in diethyl ether, and judging by similarities to compound **14** via <sup>1</sup>H NMR spectroscopy, the structures are likely analogues, yielding the proposed structure of compound **16**. Once again, it seems that a fluxional process is causing 2,3-dimethylpyrazine to appear as a broad peak in the <sup>1</sup>H NMR spectrum. Theoretically, this reaction could have resulted in a tetrametallic bridging species between two Zr centers. However, the lack of remaining starting materials and the presence of a very similar <sup>1</sup>H NMR to compound **14** suggests that 2,3-dimethylpyrazine seems to emulate the chemistry seen with pyridine and does not have the charge transfer seen with the pyrazine reaction. This provides insight because it shows that these two methyl groups are enough to disrupt the charge transfer event, which is likely due to steric interaction with the nearby mesityl groups.

With a better idea of the steric factors at hand, more appropriate pyrazine derivatives can be selected that may be able to more closely emulate the reactivity seen with pyrazine. 4,4'-

bipyridine was selected since it leaves both nitrogen atoms accessible and lacks the steric bulk of substituents on the rings. When theorizing about why the pyrazine product is unstable, it seemed possible that if it were bridging the two heterobimetallic compounds via the Zr metal centers, the mesityl groups from the two complexes would be close enough to reduce the stability of the tetrametallic species. 4,4'-bipyridine also resolves this potential issue as it would be able to effectively bridge the compounds while allowing more space between them relative to pyrazine, thus reducing strain that may be caused by steric interaction of the large mesityl groups.



**Scheme 10.** The 2:1 reaction of compound **1** and 4,4'-bipyridine in Et<sub>2</sub>O forming the proposed bridged tetrametallic compound **17**.

A 2:1 reaction of compound **1** and 4,4'-bipyridine was run in diethyl ether, which immediately turned a greenish brown and formed compound **17**. The <sup>1</sup>H NMR spectrum of the product appeared extremely similar to compound **14**, suggesting similar connectivity of the ligand. As with the pyrazine derivatives, 4,4'-bipyridine was observed as a broad peak in the aromatic region, alluding to similar fluxional behavior. The similarities show that the product is electronically comparable to compound **14**, suggesting similar connectivity. Between the spectroscopic data and the observation that no starting material remains after this 2:1 ratio reaction, it is convincing that compound **17** is a tetrametallic species that features a bridging 4,4'-bipyridine ligand. Such a species could potentially look very similar to the product of the

pyridine reaction via  $^1\text{H}$  NMR as it is structurally a dimer of compound **14**. Although the slight green coloration of the product potentially demonstrates more charge transfer than the products of other pyrazine derivatives, it fails to emulate the amount of charge transfer observed in the pyrazine reaction. This shows that simply bridging the metals with a conjugated  $\pi$ -system is insufficient to facilitate charge transfer. It is likely that the difference lies in the orbital energies of pyrazine derivatives and their ability to accept electron density.

### **Orbital Energies via Density Functional Theory Calculations**

In order to further investigate the difference in orbital energies between these compounds, calculations were conducted using density functional theory (DFT) to explore and compare the electronics of compound **14** and the analogous proposed pyrazine species (seen in Figure 5).

## Comparison of HOMO and LUMO Energies of Pyrazine and Pyridine Complexes

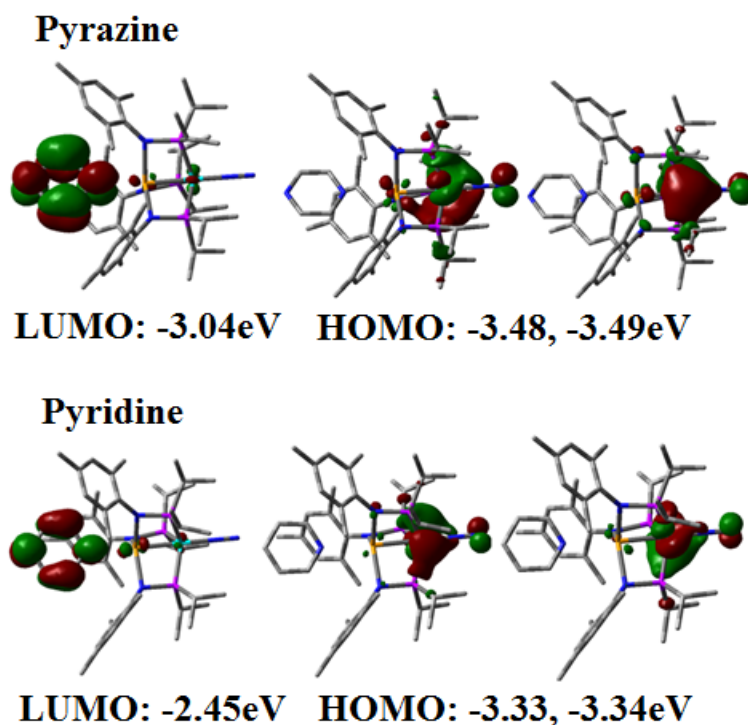


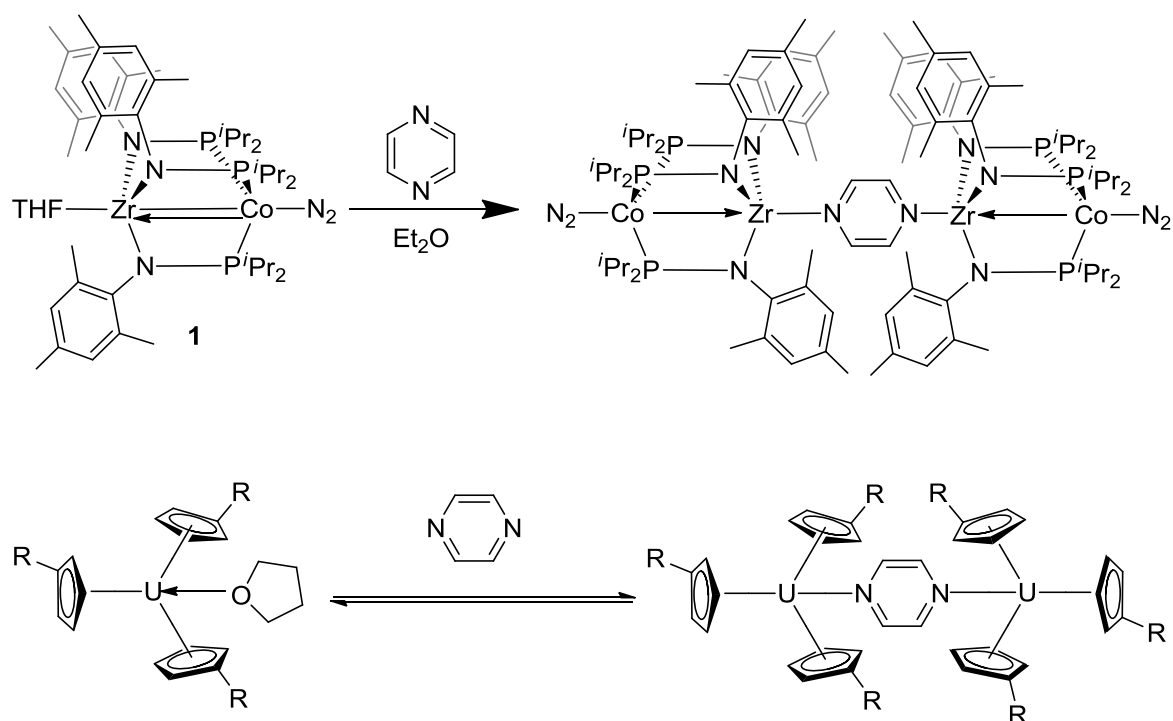
**Figure 5.** HOMO and LUMO orbitals in compound **14** and the analogous pyrazine compound and their respective orbital energies. It can be seen that the HOMO-LUMO gap is notably smaller in the pyrazine compound in comparison to the pyridine compound (**14**), which facilitates charge transfer to pyrazine. Calculated and illustrated using DFT calculations.

The calculations for the pyrazine compound show that the energy difference between the HOMOs (-3.48 eV and -3.49 eV) and the LUMO (-3.04 eV) is only 0.44 eV, which suggests that donation from the HOMOs to the LUMO has a relatively small energy barrier and could readily occur. Calculations for compound **14** (labeled pyridine in Figure 5) showed that the HOMO-(-3.33 eV and -3.34 eV) LUMO (-2.45 eV) gap is equal to 0.88 eV. The orbital energy of the pyridine is higher than that of the pyrazine, making the HOMO-LUMO gap larger and increasing the energy required to cause electron donation or charge transfer into the orbital. The LUMO of pyrazine is likely lower than pyridine because the second nitrogen in the ring draws

electron density, as it is much more electronegative relative to the carbon of pyridine. Although this explains why charge transfer is observed in the pyrazine reaction and not in the compound **14**, the structure of the pyrazine product that exhibits this charge transfer remains elusive.

### Potential Products of the Pyrazine Reaction

One likely product for the pyrazine reaction is a pyrazine-bridged tetrametallic species like the proposed structure for compound **17** and similar to the pyrazine-bridged homobimetallic uranium species shown in Scheme 10.<sup>27</sup>



**Scheme 10.** A comparison between an observed pyrazine bridged homobimetallic uranium species<sup>27</sup> and a hypothetical pyrazine bridged tetrametallic species, which is a proposed structure for the unstable product of the pyrazine reaction.

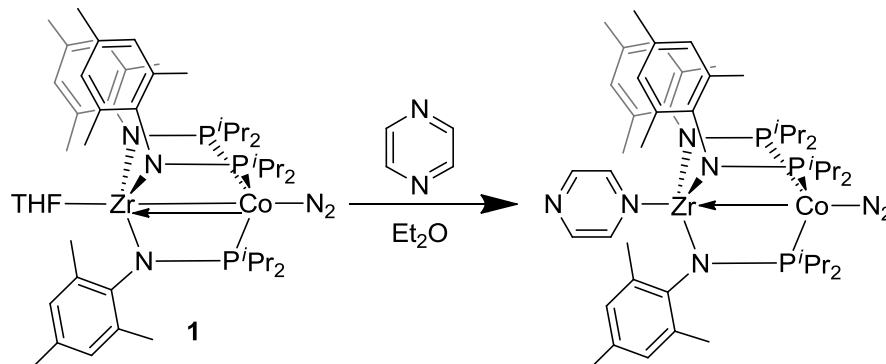
The monometallic uranium(III) species reacts with pyrazine to form a pyrazine-bridged bimetallic species that is highly colored (black)<sup>27</sup>, suggesting charge transfer. The uranium centers are likely able to donate into the low lying  $\pi$ -orbitals of pyrazine from their much higher energy orbitals in order to facilitate a large amount of charge transfer between the metal centers.

The observed uranium chemistry and proposed charge transfer suggests some comparability to the pyrazine product. With both nitrogen atoms of the pyrazine ligand available for binding and no steric interference from substituents on the heterocycle, it is reasonable to propose a structure for the pyrazine reaction that is analogous to the bimetallic uranium species. Such a species would have a significant amount of charge transfer, as electrons could potentially flow between the two bimetallic units through the pyrazine. However, a significant issue with this species is the proximity of the mesityl groups, possibly leading to instability. The steric issue would either cause the product to be unstable or prevent its formation entirely. As the observed product lacks stability, the proposed unstable structure is possibly the source of the charge transfer. Another issue with the structure is the limited comparability of the uranium chemistry from which it was derived. A uranium center features both high energy orbitals that can drive reactions with high activation energies and a sterically open environment (mostly because of its large atomic radius), which is dissimilar from the more congested environment of the Zr/Co heterobimetallic.

In addition to the largely comparable uranium-pyrazine chemistry, Mehdoui *et al.* also noted an equilibrium between pyrazine and THF in the pyrazine-bridged uranium species.<sup>27</sup> The equilibrium offers an explanation for the observation that the ligated pyrazine derivatives were only observable as broad peaks via <sup>1</sup>H NMR spectroscopy. It is likely that the NMR samples contained sufficient THF to allow for the equilibrium between pyrazine derivatives and THF to occur. The present hypothesis could be confirmed by utilizing variable temperature NMR.

In another scenario of the pyrazine reaction, where it is assumed that the steric hindrance of bridging the two Zr centers is great enough to prevent formation of the pyrazine-bridged species, a likely unstable intermediate with simple coordination to the Zr would be formed (seen

in Scheme 11).



**Scheme 11.** Ligand exchange of THF for pyrazine forms the unstable intermediate that could be the source of the observed charge transfer

The low energy  $\pi$  orbitals of pyrazine could facilitate the delocalization of electron density into the aromatic ring. The electron density would increase the reactivity of the ligand and thus reduce its stability. Under the assumption that the Zr center of another molecule is sterically inaccessible, the pyrazine would likely react with ligands causing the formation of many different products. With the limited information on the product of the pyrazine reaction, it is not possible to determine if the species that exhibits the charge transfer is the ligand exchange product, the bridged product, or another product entirely.

## Conclusion

We have reported a reaction between a Zr/Co heterobimetallic complex and pyrazine that yields a highly colored and unstable compound; the new species exhibits interesting electronic properties that may be explained by either a significant amount of charge transfer or radical chemistry. Several pyrazine derivatives were selected that would likely react similarly and yield a more stable species; however, none were able to emulate the electronic properties of the pyrazine product. Utilizing X-ray crystallography, the structure of the product of the reaction between the Zr/Co heterobimetallic complex and pyridine was obtained, revealing that pyridine had substituted for THF in a ligand-exchange reaction. By comparing the  $^1\text{H}$  NMR spectra, the products of the analogous reactions with the other pyrazine derivatives allowed for the conclusion that they were all simple ligand exchange reactions except for 4,4'-bipyridine, which was able to bridge two heterobimetallic subunits in a tetrametallic species. The identified and proposed products, especially those that came from reagents that would stabilize a radical, provide evidence against the proposed radical mechanism. Calculations were done using DFT, showing that the orbital energy of pyrazine's LUMO was lower than that of pyridine. The results demonstrate that charge transfer occurs in the pyrazine product because of its low energy  $\pi$ -orbitals, which results in a smaller HOMO-LUMO gap, facilitating the donation of electron density. There are two likely chemical scenarios in the pyrazine reaction that could create an unstable species with charge transfer: A sterically accessible Zr center allows for the formation of a pyrazine bridged tetrametallic species that electronically couples the bimetallic subunits or a sterically inaccessible Zr center that prevents bridging and leads to the formation of the ligand exchange product. With the known data, it is not possible to determine which product is responsible for the charge transfer. With further study and the use of a less bulky substituent in

place of the mesityl groups, it may be possible to isolate an analogous charge transfer species that is stable, allowing for analysis of its intriguing electronic properties.

## **Experimental**

### **General Considerations**

All reported syntheses are air or moisture sensitive and were thus performed using standard glove box techniques in the absence of water under a nitrogen atmosphere. All solvents were dried and degassed by sparging with argon gas and by passing through a column of activated alumina. These solvents were stored in the glove box under 3 Å molecular sieves to maintain dryness. Deuterated benzene was degassed using repeated freeze-pump-thaw cycles and then stored over 3 Å molecular sieves. Liquid pyrazine derivatives were degassed via sparging with nitrogen gas and were then stored in the glove box under 3 Å molecular sieves and/or alumina to maintain dryness in these hygroscopic reagents. Solid pyrazine derivatives such as acridine and 4,4-bipyridine were purified via sublimation using Schlenk technique. NMR data was collected at room temperature using a Varian Inova 400 MHz instrument. <sup>1</sup>H NMR chemical shifts were referenced to residual solvents and <sup>31</sup>P NMR chemical shifts were referenced to a 85% H<sub>3</sub>PO<sub>4</sub> standard.

### **X-Ray data collection, solution, and refinement for compound 14**

All operations were performed on a Bruker-Nonius Kappa Apex2 diffractometer, using graphite-monochromated MoK $\alpha$  radiation. All diffractometer manipulations, including data collection, integration, scaling, and absorption corrections were carried out using the Bruker Apex2 software.<sup>28</sup> Preliminary cell constants were obtained from three sets of 12 frames. Data collection was carried out at 120 K, using a frame time of 10 sec and a detector distance of 60

mm. The optimized strategy used for data collection consisted of nine phi and two omega scan sets, with  $0.5^\circ$  steps in phi or omega; completeness was 99.6 %. A total of 4169 frames were collected. Final cell constants were obtained from the xyz centroids of 9567 reflections after integration.

From the systematic absences, the observed metric constants and intensity statistics, space group  $P\bar{1}$  was chosen initially; subsequent solution and refinement confirmed the correctness of this choice. The structure was solved using *SuperFlip*,<sup>29</sup> and refined (full-matrix-least squares) using the Oxford University *Crystals for Windows* program.<sup>30</sup> The asymmetric unit contains one complex and ether molecule ( $Z = 2$ ;  $Z' = 1$ ). All non-hydrogen atoms were refined using anisotropic displacement parameters. After location of H atoms on electron-density difference maps, the H atoms were initially refined with soft restraints on the bond lengths and angles to regularize their geometry (C---H in the range 0.93--0.98 Å and  $U_{iso}$  (H) in the range 1.2-1.5 times  $U_{eq}$  of the parent atom), after which the positions were refined with riding constraints.<sup>31</sup> The final least-squares refinement converged to  $R_1 = 0.0230$  ( $I > 2\sigma(I)$ , 15017 data) and  $wR_2 = 0.0589$  ( $F^2$ , 16439 data, 595 parameters).

### Computational Details.

All calculations were performed using Gaussian09, Revision A.02 for the Linux operating system.<sup>32</sup> Density functional theory calculations were carried out using a combination of Becke's 1988 gradient-corrected exchange functional<sup>33</sup> and Perdew's 1986 electron correlation functional<sup>34</sup> (BP86). A mixed-basis set was employed, using the LANL2TZ(f) triple zeta basis set with effective core potentials for cobalt and zirconium,<sup>35</sup> Gaussian09's internal 6-311+G(d) for heteroatoms (nitrogen, oxygen, phosphorus), and Gaussian09's internal LANL2DZ basis set (equivalent to D95V)<sup>36</sup> for carbon and hydrogen. Using crystallographically determined

geometries as a starting point, the geometries were optimized to a minimum, followed by analytical frequency calculations to confirm that no imaginary frequencies were present. XYZ coordinates of optimized geometries are provided on pages S14-S18. NBO calculations were performed on the DFT-optimized geometry using NBO 3.1 as implemented in the Gaussian09 software package.<sup>37</sup>

## Procedures

**(NC<sub>5</sub>H<sub>5</sub>)Zr(NMesP<sup>i</sup>Pr<sub>2</sub>)<sub>3</sub>Co-N<sub>2</sub> (14).** Compound **1** (57.5 mg 0.0574 mmol) was dissolved in a 10 ml solution of diethyl ether and 4.6  $\mu$ l of pyridine (0.057 mmol) was added and allowed to stir for several minutes. The solution was then filtered through Celite and then the solvent was removed from the filtrate under vacuum. The product was then washed with cold pentane and dried under vacuum yielding spectroscopically pure (NC<sub>5</sub>H<sub>4</sub>)Zr(NMesP<sup>i</sup>Pr<sub>2</sub>)<sub>3</sub>Co-N<sub>2</sub> as a maroon solid (56.5 mg, 72.6% yield). Crystals suitable for X-ray diffraction were grown in a concentrated solution of diethyl ether at -35°C. <sup>1</sup>H NMR (400 MHz, C<sub>6</sub>D<sub>6</sub>):  $\delta$  6.68 (s, 6H, Mes), 6.5 (br, pyridine), 2.49 (m, 24 H, Mes-Me + CH(CH<sub>3</sub>)<sub>2</sub> overlapping), 2.08 (s, 9H, Mes-Me), 1.83 (m, 18H, CH(CH<sub>3</sub>)<sub>2</sub>), 1.58 (m, 18H, CH(CH<sub>3</sub>)<sub>2</sub>). IR (Benzene): 2045 cm<sup>-1</sup>. Note: Pyridine was likely observed as a broad peak at  $\delta$  8.2 due to fluxional exchange with trace THF.

**(NC<sub>11</sub>H<sub>9</sub>)Zr(NMesP<sup>i</sup>Pr<sub>2</sub>)<sub>3</sub>Co-N<sub>2</sub> (15).** A 2.5 ml solution of Compound **1** (6.3 mg 0.0063 mmol) in diethyl ether was added to a 2.5 ml solution of 4-phenylpyridine in diethyl ether (0.98 mg, 0.0063 mmol), instantly causing crystallization of the product. The crystals were isolated via filtration then washed with cold pentane and dried under vacuum yielding compound **15** as brown solid. <sup>1</sup>H NMR (400 MHz, C<sub>6</sub>D<sub>6</sub>):  $\delta$  6.70 (s, 6H, Mes); 2.56 (m, 18H, Mes-Me); 2.04 (s, 9H, Mes-Me); 1.85 (m, 18H, CH(CH<sub>3</sub>)<sub>2</sub>); 1.60 (m, 18H, CH(CH<sub>3</sub>)<sub>2</sub>). Note: 4-phenylpyridine was likely observed as a broad peak at  $\delta$  8.1 due to fluxional exchange with trace THF.

**(N<sub>2</sub>C<sub>6</sub>H<sub>8</sub>)Zr(NMesP<sup>i</sup>Pr<sub>2</sub>)<sub>3</sub>Co-N<sub>2</sub> (16)**. Compound **1** (34.5 mg 0.0345 mmol) was dissolved in 10 ml of diethyl ether and 3.7 μl of 2,3-dimethylpyrazine (0.034 mmol) was added and allowed to stir for several minutes. The solution was then filtered through Celite and then the solvent was removed in vacuo. The product was then washed with cold pentane and dried under vacuum affording compound **16** as a brown solid. <sup>1</sup>H NMR (400 MHz, C<sub>6</sub>D<sub>6</sub>): δ 6.76 (s, 6H, Mes); 2.44 (m, 18H, Mes-Me); 2.13 (s, 9H, Mes-Me); 1.75 (m, 18H, CH(CH<sub>3</sub>)<sub>2</sub>); 1.55 (m, 18H, CH(CH<sub>3</sub>)<sub>2</sub>). Note: 2,3-dimethylpyrazine was likely observed as a broad peak at δ 8.0 due to fluxional exchange with trace THF.

**(μ-N<sub>2</sub>C<sub>10</sub>H<sub>8</sub>)[Zr(NMesP<sup>i</sup>Pr<sub>2</sub>)<sub>3</sub>Co-N<sub>2</sub>]<sub>2</sub> (17)**. A 2.5 ml solution of compound **1** (43.9 mg 0.0439 mmol) in diethyl ether was added to a 2.5 ml diethyl ether solution containing 4,4'-bipyridine (3.5 mg, 0.022 mmol) were added to a 10 ml solution of diethyl ether and allowed to stir for several minutes. The solution was then filtered through celite and then the solvent was removed under vacuum. The product was then washed with cold pentane and dried under vacuum affording compound **17** as a greenish brown solid. <sup>1</sup>H NMR (400 MHz, C<sub>6</sub>D<sub>6</sub>): δ 6.69 (s, 6H, Mes); 2.52 (m, 18H, Mes-Me); 2.07 (s, 9H, Mes-Me); 1.82 (m, 18H, CH(CH<sub>3</sub>)<sub>2</sub>); 1.58 (m, 18H, CH(CH<sub>3</sub>)<sub>2</sub>). Note: 4,4'-bipyridine was likely observed as a broad peak at δ 7.8 due to fluxional exchange with trace THF.

## References

- <sup>1</sup>Pérez-Temprano, M. H.; Casares, J. A.; Espinet, P. *Chem. Eur. J.* **2012**, *18*, 1864-1884.
- <sup>2</sup>Wheatley, N.; Kalck, P. *Chem. Rev.* **1999**, *99*, 3379-3420.
- <sup>3</sup>Thomas, C. M. *Comments Inorg. Chem.* **2011**, *32*, 14-38.
- <sup>4</sup>Cooper, B. G.; Napoline, J. W.; Thomas, C. M. *Cat. Rev. -Sci. Eng.* **2012**, *54*, 1-40.
- <sup>5</sup>Nagashima, H.; Sue, T.; Oda, T.; Kanemitsu, A.; Matsumoto, T.; Motoyama, Y.; Sunada, Y. *Organometallics* **2006**, *25* (8), 1987-1994.
- <sup>6</sup>Sunada, Y.; Sue, T.; Matsumoto, T.; Nagashima, H. *J. Organomet. Chem.* **2006**, *691* (14), 3176-3182.
- <sup>7</sup>Greenwood, B. P.; Rowe, G. T.; Chen, C.H.; Foxman, B. M.; Thomas, C. M. *J. Am. Chem. Soc.* **2010**, *132*, 44-45.
- <sup>8</sup>Cordero, B.; Gómez, V.; Platero-Prats, A.; Revés, M.; Echeverría, J.; Cremades, E.; Barragán, F.; Alvarez, S. *Royal Soc. Chem.* **2008**, *21*, 2832-2838
- <sup>9</sup>Krogman, J. P.; Foxman B. M.; Thomas, C. M. *J. Am. Chem. Soc.* **2011**, *133*, 14582-14585.
- <sup>10</sup>Thomas, C. M.; Napoline, J. W.; Rowe, G. T.; Foxman, B. M. *Chem. Commun.* **2010**, *46*, 5790-5792.
- <sup>11</sup>Napoline, J. W.; Bezpalko, M. W.; Foxman B. M.; Thomas, C. M. *Chem. Commun.* **2013**, *49*, 4388-4390.
- <sup>12</sup>Zhou, W.; Napoline, J. W.; Thomas, C. M. *Eur. J. Inorg. Chem.* **2011**, *2011*, 2029-2033.
- <sup>13</sup>Darwent B. National Standard Reference Data System. The Catholic University of America, **1970**.
- <sup>14</sup>Gross, R.; Kaim, W. *Inorg. Chem.* **1986**, *25*, 498-506.
- <sup>15</sup>Modéc, B.; Šala, M.; Clérac, R. *Eur. J. Inorg. Chem.* **2010**, *2010*, 542-553.
- <sup>16</sup>Wriedt, M.; Jeß, I.; Näther, C. *Eur. J. Inorg. Chem.* **2009**, *2009*, 1406-1413.
- <sup>17</sup>Zhang, L.; Fakhouri, S. M.; Liu, F.; Timmons, J. C.; Ran, N. A.; Briseno, A. L. *J. Mater. Chem.* **2011**, *21*, 1329-1337.
- <sup>18</sup>Demadi, K. D.; Hartshorn, C. M.; Meyer, T. J. *Chem. Rev.* **2001**, *101*, 2655.
- <sup>19</sup>Creutz, C.; Taube, H. *J. Am. Chem. Soc.* **1969**, *91*, 3988.
- <sup>20</sup>Creutz, C.; Taube, H. *J. Am. Chem. Soc.* **1973**, *95*, 1086.
- <sup>21</sup>Kaim, W. *Anorganische Chemie*, **1981**, *36*, 1110-16.
- <sup>22</sup>Kaim, W. *Inorg. Chim. Acta.* **1981**, *53*, 151-153.
- <sup>23</sup>Zhou, W.; Marquard, S. L.; Bezpalko, M. W.; Foxman, B. M.; Thomas, C. M. *Organometallics*, **2013**, *32*, 1766-1772.
- <sup>24</sup>Mendiratta, A.; Cummins, C. C. *Inorg. Chem.* **2005**, *44*, 7319-7321.
- <sup>25</sup>Lancaster, S. J.; Hughes, D. L. *Dalton Trans.* **2003**, 1779.
- <sup>26</sup>Fischer, R.; Walther, D.; Gebhardt, P.; Górls, H. *Organometallics.* **2000**, *19*, 2532.
- <sup>27</sup>Mehdoui, T.; Berthet, J.; Thuéry, P.; Ephritikhine, M. *Eur. J. Inorg Chem.* **2004**, *2004*, 10, 1996-2000.
- <sup>28</sup>Apex2, Version 2 User Manual, M86-E01078, Bruker Analytical X-ray Systems, Madison, WI, June 2006.
- <sup>29</sup>Palatinus, L.; Chapuis, G.; *J. Appl. Cryst.* **2007**, *40*, 786.
- <sup>30</sup>Betteridge, P. W.; Carruthers, J. R.; Cooper, R. I.; Prout, K.; Watkin, D. J. *J. Appl. Cryst.* **2003**, *36*, 1487; Prout, C.K.; Pearce, L.J. CAMERON, Chemical Crystallography Laboratory, Oxford, UK, 1996.
- <sup>31</sup>Cooper, R. I.; Thompson, A. L.; Watkin, D. J. *J. Appl. Cryst.* **2010**, *43*, 1100-1107.

- <sup>32</sup> Frisch, M. J.; Trucks, G. W.; Schlegel, H. B.; Scuseria, G. E.; Robb, M. A.; Cheeseman, J. R.; Scalmani, G.; Barone, V.; Mennucci, B.; Petersson, G. A.; Nakatsuji, H.; Caricato, M.; Li, X.; Hratchian, H. P.; Izmaylov, A. F.; Bloino, J.; Zheng, G.; Sonnenberg, J. L.; Hada, M.; Ehara, M.; Toyota, K.; Fukuda, R.; Hasegawa, J.; Ishida, M.; Nakajima, T.; Honda, Y.; Kitao, O.; Nakai, H.; Vreven, T.; Montgomery Jr., J. A.; Peralta, J. E.; Ogliaro, F.; Bearpark, M.; Heyd, J. J.; Brothers, E.; Kudin, K. N.; Staroverov, V. N.; Kobayashi, R.; Normand, J.; Raghavachari, K.; Rendell, A.; Burant, J. C.; Iyengar, S. S.; Tomasi, J.; Cossi, M.; Rega, N.; Millam, J. M.; Klene, M.; Knox, J. E.; Cross, J. B.; Bakken, V.; Adamo, C.; Jaramillo, J.; Gomperts, R.; Stratmann, R. E.; Yazyev, O.; Austin, A. J.; Cammi, R.; Pomelli, C.; Ochterski, J. W.; Martin, R. L.; Morokuma, K.; Zakrzewski, V. G.; Voth, G. A.; Salvador, P.; Dannenberg, J. J.; Dapprich, S.; Daniels, A. D.; Farkas, O.; Foresman, J. B.; Ortiz, J. V.; Cioslowski, J.; Fox, D. J., Gaussian, Inc., Wallingford, CT, **2009**.
- <sup>33</sup> Becke, A. D. *Phys. Rev. A* **1988**, *38*, 3098.
- <sup>34</sup> Perdew, J. P. *Physical Review B* **1986**, *33*, 8822.
- <sup>35</sup> (a) Hay, P. J.; Wadt, W. R. *J. Chem. Phys.* **1985**, *82*, 299. (b) Hay, P. J.; Wadt, W. R. *J. Chem. Phys.* **1985**, *82*, 270.
- <sup>36</sup> Dunning, T. H.; Hay, P. J. *Modern Theoretical Chemistry*. Vol. 3, Plenum, New York, **1976**.
- <sup>37</sup> Glendening, E. D.; Reed, A. E.; Carpenter, J. E. *NBO Version 3.1*